other conditions for providing a system circuit flow and keeping "hot spots" from occurring, it is anticipated that the hydraulic system would probably use a series of bleeds. That is, high-pressure fluid is diverted to the low-pressure side to produce system circulation.

Usually $\frac{1}{4}$ to $\frac{1}{2}$ gpm flows are sufficient to accomplish the desired system temperature stabilizations. These system bleeds are now being used in certain present subsonic turbine-powered aircraft.

Although some present high-temperature systems are using the MLO-8200 series of fluids, it is felt that these disiloxane based fluids have lower lubricity values than the petroleum based fluids.

More than 4000 hr of operation have been conducted in laboratory tests with the MLO-7277 fluid in the 550°F range. Of this time, more than 250 hr were conducted on one test pump. The fluid used for this high-speed transport will be required to have thermal stability, inasmuch as there may be as many as four thermal cycles, or four Mach 3 flights/24-hr period. Care must be given to eliminate both air and water from the system to provide the correct system response and eliminate any possibility of "spongy" system operation.

System Filtration

Studies of the Commercial Jet Hydraulic Systems Panel during the past 2 years have indicated very great benefit from added system filtration. This has been both in respect to over-all system reliability as well as general efficiency of system operation. In present commercial jet aircraft, a number of filters have been added to the pump case drain and return system lines.

Studies have also indicated that certain advantages are gained from relying on the airborne system filters for cleaning up system with no outside flushing. During the past few years considerable difficulty has been experienced with trying to clean up certain systems by using ground carts for flushing purposes. At times more contaminant is put into the system than removed from the system.

Tubing and Fittings

It is anticipated that most of the tubing and fitting material will be of a stainless steel high-strength alloy. As in the case of both the Lockheed Electra investigational programs and the present B-70 design, it is anticipated that tubing connections will be minimized with connections made through manifolds. This is largely because of a reliability aspect in reducing the leakage areas, but also results in considerable saving to the aircraft weight, possibly as much as several thousand pounds.

Conclusion

The results of the past studies on commercial jet hydraulic systems have proved extremely beneficial in the nature of optimizing hydraulic system operations. With this continued monitoring and study with additional specialized studies in specific areas, prior to the end of this decade supersonic commercial jet transport will probably be seen playing a major effort in airline transportation industry.

JANUARY-FEBRUARY 1964 J. AIRCRAFT VOL. 1, NO. 1

Analytical Method for Designing Turbine Nozzle Partitions

DONALD J. DUSA *
General Electric Company, Cincinnati, Ohio

AND

WIDEN TABAKOFF†
University of Cincinnati, Cincinnati, Ohio

An analytical method of determining the blade shape of turbine nozzle partitions and stationary blades for subsonic flow is presented in this work. Two important advantages over the present design methods are noted, namely: The initial design and the iterations to the desired blade shape can be done by a computing machine, and the profile of the suction and pressure surfaces can be described by a continuous curve from the leading edge tangent point to the trailing edge.

Nomenclature‡

θ_E = inlet angle
θ_X = exit angle
θ_1 = suction surface exit angle
θ_2 = suction surface inlet angle
θ_4 = pressure surface exit angle
θ_5 = pressure surface inlet angle
θ_3 = angle of slope at throat
θ_{te} = trailing edge wedge angle, 6.5°
θ_{le} = leading edge wedge angle, 31.0°
θ_6 = θ_3
θ_7 = θ_5
TET = trailing edge thickness
XER = leading edge radius
DT = nozzle throat width
W = blade width
H = blade height
P = blade pitch
L = $W - XER$

Received July 11, 1963; revision received October 28, 1963.
* Engineer, Aero-Thermo Design. Associate Member AIAA.
† Associate Professor. Member AIAA.
‡ Definition of symbols for Fig. 2.

Introduction

ONE of the present methods of designing turbine nozzle partitions is to lay out the blade shape, based on cycle data and structural requirements, and then analyze the flow field to determine the velocity and pressure profiles

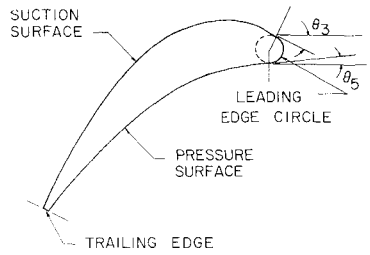

Fig. 1 Turbine nozzle partition.

through the cascade. This is essentially an iterative process through which an attempt is made to satisfy both the aerodynamic and structural requirements.

At the present, there are approximately three standard methods of specifying the blade profile.[1] Of these, the most widespread method is to specify the coordinates about the profile. The coordinates are determined by drawing the blade freehand based on experience.

Because of the general shape of the blade, it was thought that nozzle partitions could be described analytically. The advantages of describing the profile analytically are that the initial design and iterations to the desired blade shape can be done by a computing machine, and that the profile of the suction and pressure surfaces can be described by a continuous curve from the leading edge tangent point to the trailing edge. The advantage of the computing machine is obvious, and the continuity of the blade profile is very desirable for the fluid analysis. Several methods were tried, but the one described in this work was found to be the most favorable.

Scope

The scope of this work is best described by Fig. 1, in which the general blade shape of a turbine nozzle partition is given, along with the basic assumptions and considerations shown below.

The suction surface is considered to be generated by a general second-degree conic equation of the form

$$x^2 + Bxy + Cy^2 + Dx + Ey + F = 0$$

The pressure surface is considered to be generated by a general second-degree elliptical equation of the form

$$x^2 + By^2 + Cx + Dy + E = 0$$

The leading edge is circular. The trailing edge is squared off and assumed perpendicular to the suction surface. The angle, where the suction surface is tangent to the leading edge circle, θ_3 is limited: $\theta_3 < 0°$. The angle, where the pressure surface is tangent to the leading edge circle, θ_5 is limited: $\theta_5 > 0°$.

Requirements

Some boundary conditions and parameters are required in order to arrive at a solution for the suction and pressure surface equations. The boundary conditions outlined below, with reference to Fig. 2, were found to be the most favorable for the analysis.

Suction surface boundary conditions:

1) x and y coordinates at ①
2) x and y corrdinates at ②
3) slope at ②
4) x and y coordinates at ③
5) slope at ③

Pressure surface boundary conditions:

1) x and y coordinates at ④
2) slope at ④
3) x and y coordinates at ⑤
4) slope at ⑤

A factor affecting the choice of the foregoing equations for the suction and pressure surfaces was the limited number of boundary conditions that could be determined, with a fair amount of consistency, from a general study. It was found that no more than three sets of coordinates and the slopes of each set could be determined in general for the suction surface, and that two sets of coordinates and the slopes of each set could be determined in general for the pressure surface.

Method of Solution

In order to determine the prescribed boundary conditions, it is necessary to derive some general criterion that would be applicable to any nozzle partition (see Fig. 2). The initial conditions, determined from cycle analysis and structural requirements, which are usually known prior to designing the blade regardless of the method used to design it, are tabulated as θ_E, θ_X, XER, TET, W, DT, and P.

An investigation of several nozzle partitions currently in use and a general knowledge of the state of the art yielded the following relationships applicable to root, pitch, and tip sections.

The angle of overturn, $\theta_1 - \theta_X$, ranges from approximately 1.5° to 2.5°.

The trailing edge wedge angle θ_{te} was found to average approximately 6.5°.

The suction surface leading edge tangent angle θ_3 was found to vary as a function of the inlet angle θ_E; a curve of this relationship is shown on Fig. 3 for inlet angles between 0.0° and −20.0°.

The leading edge wedge angle, the sum of the suction and pressure surface leading edge tangent angles, $(\theta_5 + |\theta_3|)$, was found to average approximately 31.0°.

The unguided turning, $\theta_X - \theta_2$, which ranges from about 7.0° to 12.0°, was found to vary as a function of exit angle and is plotted vs exit angle on Fig. 4.

The stagger angle, defined here as the angle between a horizontal line through the trailing edge of the suction surface and a line from the trailing edge of the suction surface to the center of the leading edge circle, was found to vary as a func-

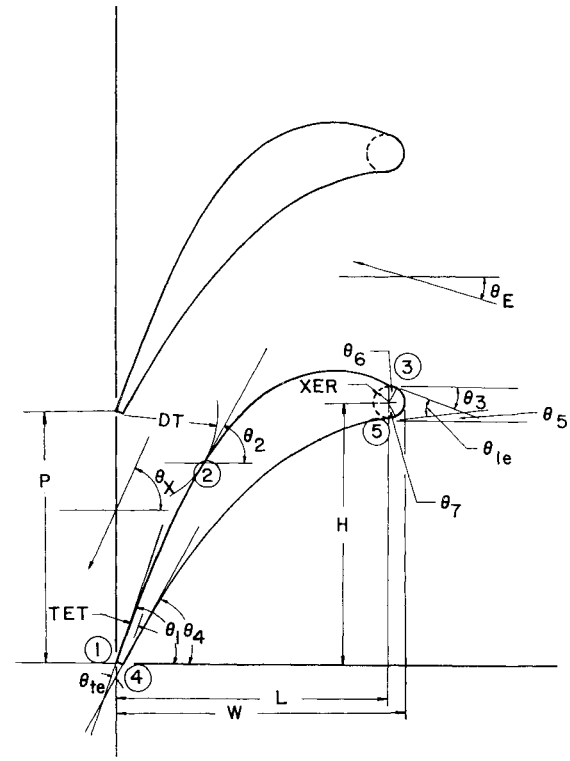

Fig. 2 Description of boundary conditions and parameters.

tion of the tangents of the inlet and exit angles. The slope of the stagger angle H/L, where L is the blade width minus the leading edge radius ($W - XER$), is plotted vs $(\tan\theta_X - |\tan\theta_E|)/2$ on Fig. 5.

Using the foregoing relationships, the solution of the boundary conditions, for the suction and pressure surfaces, is tabulated in the following sections (see the Appendix for a complete example problem).

Suction Surface Boundary Conditions

1) x and y coordinates at ①: Assume as origin; $x = 0$, $y = 0$.

2) x and y coordinates at ②: This set of coordinates may be calculated from the geometry of the nozzle by use of θ_1, TET, P, DT, and θ_2.

3) Slope at ②: θ_2 is determined from the curve of $(\theta_X - \theta_2)$ vs θ_X (Fig. 4).

4) x and y coordinates at ③: This set of coordinates is calculated from the geometry of the nozzle by use of XER, H, L, and θ_3. H is found from the curve of H/L vs $(\tan\theta_X - |\tan\theta_E|)/2$ (Fig. 5).

5) Slope at ③: θ_3 is determined from the curve θ_3 vs θ_E (Fig. 3).

Pressure Surface Boundary Conditions

1) x and y coordinates at ④: This set of coordinates is calculated from the geometry of the nozzle by use of TET and θ_1.

2) Slope at ④: $\theta_4 = \theta_1 - 6.5°$.

3) x and y coordinates at ⑤: This set of coordinates may be calculated from the geometry of the nozzle by use of XER, H, L, and θ_5.

4) Slope at ⑤: $\theta_5 = 31.0° - \theta_3$.

Using the foregoing boundary conditions, five equations with five unknowns may be written for the suction surface, and four equations with four unknowns may be written for the pressure surface. Noting that the derivative dy/dx expresses the tangent of the slope at any point along the surface, the simultaneous equations may be written as shown next.

Simultaneous Equations for Suction Surface

$$x^2 + Bxy + Cy^2 + Dx + Ey + F = 0$$

$$d(\ )/dx = 2x + (y + x\,dy/dx)B + (2y\ dy/dx)C + D + (dy/dx)E = 0$$

At $x = x_1 = 0$, $y = y_1 = 0$:

$$F = 0$$

At $x = x_2$, $y = y_2$:

$$x_2^2 + x_2y_2B + y_2^2C + x_2D + y_2E = 0$$

At $x = x_2$, $y = y_2$, $dy/dx = \tan\theta_2$:

$$2x_2 + (y_2 + x_2\tan\theta_2)B + (2y_2\tan\theta_2)C + D + (\tan\theta_2)E = 0$$

At $x = x_3$, $y = y_3$:

$$x_3^2 + x_3y_3B + y_3^2C + x_3D + y_3E = 0$$

At $x = x_3$, $y = y_3$, $dy/dx = \tan\theta_3$:

$$2x_3 + (y_3 + x_3\tan\theta_3)B + (2y_3\tan\theta_3)C + D + (\tan\theta_3)E = 0$$

Simultaneous Equations for Pressure Surface

$$x^2 + By^2 + Cx + Dy + E = 0$$

$$d(\ )/dx = 2x + (2ydy/dx)B + C + (dy/dx)D = 0$$

At $x = x_4$, $y = y_4$:

$$x_4^2 + y_4^2B + x_4C + y_4D + E = 0$$

At $x = x_4$, $y = y_4$, $dy/dx = \tan\theta_4$:

$$2x_4 + (2y_4\tan\theta_4)B + C + (\tan\theta_4)D = 0$$

At $x = x_5$, $y = y_5$:

$$x_5^2 + y_5^2B + x_5C + y_5D + E = 0$$

At $x = x_5$, $y = y_5$, $dy/dx = \tan\theta_5$:

$$2x_5 + (2y_5\tan\theta_5)B + C + (\tan\theta_5)D = 0$$

The foregoing subscripted values are those determined from the previous discussion and are presented in the Appendix for a particular example. The solution of the foregoing two sets of simultaneous equations may be worked out by substitution, determinants, or matrices, and can be accomplished very easily on a computing machine. Thus, with the determination of the constants in the suction and pressure surface equations, the coordinates may be specified at any desired location around the entire blade. In addition to the coordinates, the slope, radius of curvature, and surface distance may also be specified around the blade with the assurance of continuity, which is important for the fluid analysis.

It should be pointed out at this time that the boundary conditions used for the solution to the forementioned equations are by no means rigorous values; they are used primarily in an attempt to obtain a good first approximation for the blade shape. It is assumed that the experience of the design engineer is sufficient to dictate any required changes in the boundary conditions. This iterative process is feasible considering that it takes approximately 18 sec of machine time (based on IBM 7090) to run the program of this study. Therefore, after the first approximation several runs, incorporating various alterations, may be made simultaneously, thus shortening the design time.

Results and Discussion

The method described in this study was used in an attempt to duplicate a previously designed turbine nozzle partition (Fig. 6). The comparison is quite favorable and is typical of several comparisons made with previously designed blades.

The boundary conditions used to determine the analytical comparison were taken directly from the designed blade because a direct comparison was desired; nevertheless, the same analytical profile could have been determined by an iterative process. The greater curvature of the analytical blade between the throat and leading edge of the suction surface is indicative of all the comparisons made.

Changing the boundary conditions has the following effect on the blade shape, assuming the blade height H to be constant:

1) The angle θ_1 essentially has no effect on the shape of the profile, as it is used only to determine the coordinate location

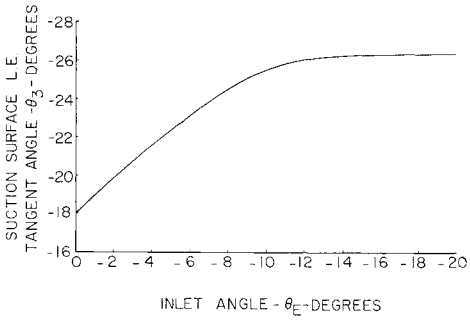

Fig. 3 Inlet angle vs suction surface leading edge tangent angle.

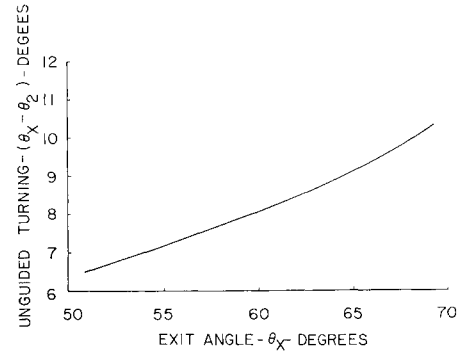

Fig. 4 Exit angle vs unguided turning.

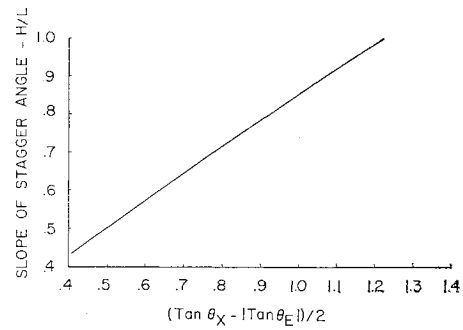

Fig. 5 Stagger angle vs parameter of $(\tan\theta_x - |\tan\theta_E|)/2$.

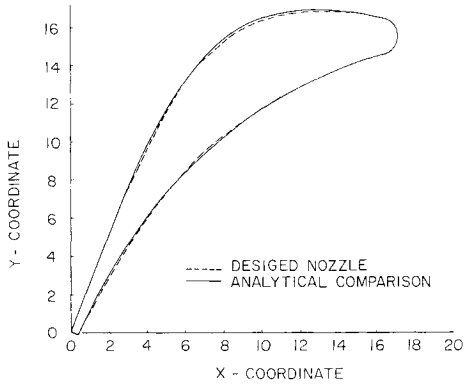

Fig. 6 Turbine nozzle partition—analytical comparison with a previously designed blade.

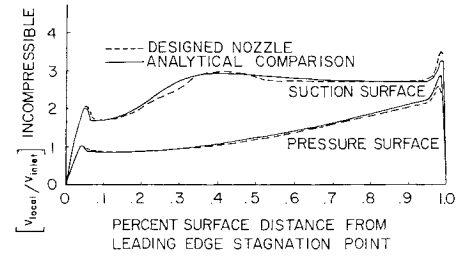

Fig. 7 Turbine nozzle partition-velocity distribution vs percent surface distance.

of the trailing edge of the pressure surface. The actual slope at the trailing edge of the suction surface does approximate this angle very closely.

2) Increasing the slope at the throat of the suction surface θ_2 will increase the curvature between the throat and leading edge and decrease the curvature from the throat to the trailing edge of the suction surface. The opposite applies for a decrease in θ_2. The shape between the throat and leading edge is the most affected, and a change of $\pm 0.25°$ at a time is the order of magnitude suggested for iterative purposes.

3) Decreasing θ_3 (less negative) decreases the curvature at the leading edge of the suction surface, but incresaes the curvature before the throat. An increase in θ_3 has the opposite effect. For this angle, a change of one or several degrees at a time is suggested for iterative purposes.

4) The effect on the curvature of the pressure surface by changing θ_4 and θ_5 is obvious, and a change of one or several degrees at a time is again suggested for iterative purposes.

Figure 7 shows the incompressible velocity distribution over the surface of a previously designed blade and its analytical comparison (Fig. 6). The velocity distribution was calculated by a computer using a cascade, potential flow analysis. It is obvious, from an inspection of Fig. 7, that the velocity distribution is much smoother for the analytical comparison than for the previously designed blade, since the curvature is much smoother due to the continuity of the analytically designed blade. Figures 6 and 7 demonstrate the ability of the method to produce a desirable blade.

Appendix

The following discussion encompasses a complete example in order to demonstrate the method analytically. From a cycle analysis and structural requirements the following initial conditions are assumed to be known for a particular turbine nozzle partition root section (Fig. 2):

inlet angle $\theta_E = -8.8°$
exit angle $\theta_X = 68.39°$
leading edge radius $XER = 0.90$ in.
trailing edge thickness $TET = 0.40$ in.
blade width $W = 15.0$ in.
nozzle throat width $DT = 4.905$ in.
pitch $P = 13.18$ in.

The linear dimensions are all ten times size for practical reasons.

Suction Surface Boundary Conditions

1) x and y coordinates at ①:
Assume as origin $x_1 = 0$, $y_1 = 0$.
2) x and y coordinates at ②:
$\theta_1 = \theta_X + 2.0° = 70.39°$
$\theta_2 = 58.39°$ (Fig. 4)
$x_2 = TET \sin\theta_1 + DT \sin\theta_2$
$= (0.4) \sin 70.39° + 4.905 \sin 58.39° = 4.55456$
$y_2 = P - TET \cos\theta_1 - DT \cos\theta_2$
$= 13.18 - (0.4) \cos 70.39° - 4.905 \cos 58.39° = 10.47565$
3) Slope at ②:
$\theta_X - \theta_2 = 10°$ (Fig. 4)
$\theta_2 = \theta_X - 10° = 58.39°$
4) x and y coordinates at ③:
$\theta_3 = -25.0°$ (Fig. 3)
$(\tan\theta_x - |\tan\theta_E|)/2 = 1.19208$

$H/L = 0.975$ (Fig. 5)
$L = W - DT = 14.1$
$H = (0.975)L = 13.75$
$x_3 = W - XER + XER \sin\theta_3$
$= 15.0 - 0.9(1 - \sin 25°) = 14.48036$
$y_3 = H + XER \cos\theta_3$
$= 13.75 + 0.9 \cos 25° = 14.568$
5) Slope at ③:
$\theta_3 = -25.0°$ (Fig. 3)

Pressure Surface Boundary Conditions

1) x and y coordinates at ④:
$x_4 = TET \sin\theta_1$
$= (0.4) \sin 70.39° = 0.37682$
$y_4 = -TET \cos\theta_1$
$= -(0.4) \cos 70.39° = -0.13418$
2) Slope at ④:
$\theta_4 = \theta_1 - 6.5° = 63.86°$
3) x and y coordinates at ⑤:
$\theta_5 = 31.0° - \theta_3 = 6°$
$x_5 = W - XER + XER \sin\theta_5$
$= 15.0 - 0.9(1 - \sin 6°) = 14.19408$
$y_5 = H - XER \cos\theta_5$
$= 13.75 - (0.9) \cos 6° = 12.85492$
4) Slope at ⑤:
$\theta_5 = 31.0° - \theta_3 = 6°$

Using the foregoing boundary conditions with the corresponding equations for the suction and pressure surfaces yields the following solution for the coefficients.

Suction surface:

$B = 0.47078$
$C = -0.12464$
$D = -29.63788$
$E = 10.06706$
$F = 0$
$x^2 + (0.47078)xy + (-0.12464)y^2 + (-29.63788)x + (10.06706)y = 0$

Pressure surface:

$B = 0.17614$
$C = -30.39820$
$D = 14.59569$
$E = 13.26829$
$x^2 + (0.17614)y^2 + (-30.39820)x + (14.59569)y + 13.26829 = 0$

Once the values for the coefficients have been determined, the curve properties are calculated routinely.

Reference

[1] Deich, M. E., "Flow of gas through turbine latices," English transl., NACA TM 1393, Washington, D. C. (May 1956).

JANUARY-FEBRUARY 1964 J. AIRCRAFT VOL. 1, NO. 1

Design Optimization of Aircraft Structures with Thermal Gradients

LLOYD E. HACKMAN* AND JAMES E. RICHARDSON†
North American Aviation, Inc., Columbus, Ohio

A technique of optimizing a structure subjected to a thermal gradient has been developed. The derivation of optimization equations is demonstrated for three types of basic structure: 1) a honeycomb compression panel, 2) a skin-stringer compression element, and 3) an *I*-beam section. The optimization on these typical structural elements is performed maintaining the interdependency of the structural configuration and the temperature distribution. The procedures also maintain such variables as material properties and a nonlinear stress-strain relation. The complexity of the applied stress and allowable equations has dictated a change in approach of the optimization problem to one of allowable and applied strains rather than allowable and applied stresses. It must be concluded from the results of this optimum design study that it is feasible to account for thermal stress and temperature effects in the preliminary design stages of an aircraft structure.

Nomenclature

A	=	defined by Eq. (2)
A_S, A_T, A_L, A_F, A_n	=	area, in.^{2}
a	=	width of panel, loaded edge, in.
b	=	length of panel, unloaded edge, in.
b_s	=	stringer spacing, in.
C	=	core depth, in.
C_s	=	effective area coefficient
c_1, c_2, c_3, c_4	=	edge fixity constants, Ref. 1
CL	=	cord length, in.
E	=	Young's modulus, psi
e	=	strain, in./in.
F	=	panel buckling constant
F_{ci}	=	intercell buckling stress, psi
F_c	=	compression stress, psi
F_t	=	tension stress, psi
F_y	=	yield stress, psi
G_c'	=	effective core shear modulus, psi
h	=	stringer, depth, in.
K	=	panel buckling constant
K_T	=	thermal constant, °F-in.
L	=	panel buckling constant
L_c	=	column length, in.
m	=	Ramberg-Osgood coefficient
M_u	=	applied bending moment, in./lb
P	=	applied axial load, lb/in.
P_A, P_{cc}, P_s	=	axial load, lb
Q	=	applied shear load, lb
S	=	core cell size, in.
t	=	thickness, in.
t_f	=	honeycomb panel facing, in.
t_c	=	core foil thickness, in.
T	=	temperature, °F
T_B	=	boundary-layer temperature, °F
V_x, V_y	=	core shear stiffness parameter
y, y_n	=	element distance from a given axis, in.
μ	=	Poisson's ratio
α	=	coefficient of expansion, in./°F-in.

Subscripts

b	=	stringer
c	=	core
cc	=	crippling
cR	=	critical buckling stress
cy	=	compression yield
f	=	facing
L	=	lower
n	=	generalize element number
R	=	effective modulus
s	=	secant, skin
T	=	tangent
u	=	upper, ultimate
w	=	web
x	=	component in x direction
y	=	component in y direction
1	=	hot facing of honeycomb panel
2	=	cold facing of honeycomb panel

Presented as Preprint 63-9 at the IAS 31st Annual Meeting, New York, January 21–23, 1963; revision received September 27, 1963.

* Specialist, Structural Mechanics Research and Development Section. Member AIAA.

† Engineer, Structural Mechanics Research and Development Section; now in Structures Group, Liquid Rocket Plant, Aerojet General, Sacramento, Calif.